LETTERS

Crustal rheology of the Himalaya and Southern Tibet inferred from magnetotelluric data

M. J. Unsworth[1], A. G. Jones[2], W. Wei[3], G. Marquis[4], S. G. Gokarn[5], J. E. Spratt[2] & the INDEPTH-MT team*

The Cenozoic collision between the Indian and Asian continents formed the Tibetan plateau, beginning about 70 million years ago. Since this time, at least 1,400 km of convergence has been accommodated[1] by a combination of underthrusting of Indian[2] and Asian lithosphere, crustal shortening[3], horizontal extrusion[4] and lithospheric delamination[5]. Rocks exposed in the Himalaya show evidence of crustal melting[1,6] and are thought to have been exhumed by rapid erosion and climatically forced crustal flow[7,8]. Magnetotelluric data can be used to image subsurface electrical resistivity, a parameter sensitive to the presence of interconnected fluids in the host rock matrix, even at low volume fractions. Here we present magnetotelluric data from the Tibetan–Himalayan orogen from 77° E to 92° E, which show that low resistivity, interpreted as a partially molten layer, is present along at least 1,000 km of the southern margin of the Tibetan plateau. The inferred low viscosity of this layer is consistent with the development of climatically forced crustal flow in Southern Tibet.

The geology of southern Tibet clearly records the collision of India with Asia. The Indus–Tsangpo suture divides rocks of Indian and Asian origin, and the Gandese batholith to the north is a consequence of pre-collision subduction of Indian lithosphere[1]. The Tethyan Himalaya to the south of the Indus–Tsangpo suture is a fold-and-thrust sequence comprising low-grade meta-sedimentary rocks deposited on the Indian continental margin of the Tethys Ocean before collision[1]. In the central Tethyan Himalaya, basement windows expose gneissic domes composed of metamorphic basement rocks and small volumes of Cenozoic granitoids produced by crustal melting[9]. To the south of the Tethyan Himalaya is the Greater Himalayan Sequence composed primarily of high-grade gneisses and bounded on its upper surface by the South Tibetan detachment. The South Tibetan detachment is essentially a normal fault that places Tethyan rocks above the Greater Himalayan Sequence. The lower boundary of the Greater Himalayan Sequence is the Main Central Thrust—a largely inactive thrust whose role in orogenic convergence has been superseded by the Main Boundary Thrust and Main Frontal Thrust. The Greater Himalayan Sequence contains pervasive migmatites and is frequently intruded at the top by leucogranites that represent the product of Miocene crustal melting. Crustal melting and the extruded metamorphic slab, bounded between the Main Central Thrust and South Tibetan detachment, show that mid-crustal rocks have been exhumed in the Himalaya[6,7]. In the northwest Himalaya the geology is similar, and the same major structural units found in southern Tibet are also present. In contrast to southern Tibet, convergence has been significantly transpressional, as expressed in the 150-km right lateral offset of the Karakorum fault[1].

Geophysical imaging in the Himalaya and Tibet has extended these surface geological studies to depth. Passive seismic data reveal a crustal thickness of up to 85 km in southern Tibet[10], approximately double the global average. Seismic reflection data demonstrate that in southern Tibet this double thickness is the result of underthrusting by the Indian plate[11]. Seismic surveys also detected bright spots that suggest a fluid phase is present at mid-crustal depths[11]. To determine whether widespread crustal flow is occurring, information about crustal composition and rheology is required and can be inferred from complementary geophysical methods such as magnetotellurics (MT). The first MT data collected in southern Tibet detected a low-resistivity crust[12]. In combination with increased heat flow[13], it was proposed that the low resistivity was due to partial melting. INDEPTH MT data collected in 1995 and 1998 showed that the low-resistivity layer extended north from 29° N into the Lhasa block[14]. However, the INDEPTH survey in Southern Tibet was located within the Yadong–Gulu rift system, part of a series of Neogene rifts that accommodates east–west extension[15], and it was uncertain whether the resistivity models were valid for the entire Tibetan–Himalayan orogen.

New long-period (0.05–0.0001 Hz) and broadband (300–0.001 Hz) INDEPTH MT data were collected in 2001 on the 700 and 800 lines (Fig. 1). The time series data were processed using statistically robust algorithms[16]. Where long-period data were available they were merged with the broadband data. The 800-line data were combined with data collected in Nepal[17] to give a profile extending from Nepal to Central Tibet, and MT data from the northwest Himalaya of India[18] have also been analysed. Tensor decomposition[19] of the MT impedance tensors shows that the geoelectric strike is parallel to geologic strike and justifies a two-dimensional analysis (Fig. 1). The apparent resistivity decreases at frequencies below 1 Hz both north and south of the Indus–Tsangpo suture. Decreasing frequency in MT indicates an increasing depth of signal penetration. Thus this observation shows that, to first order, a low-resistivity layer is present over a significant area of southern Tibet. Representative apparent resistivity curves are shown in the online supplement.

To interpret these MT data quantitatively, it is necessary to convert frequency to depth. The electrical resistivity models shown in Fig. 2 were obtained by joint inversion of the transverse magnetic mode (electric current flow along profile) and the vertical magnetic field transfer functions with an automated algorithm[20]. The fit of the inversion models responses to the measured MT data are shown in the Supplementary Information. A crustal low-resistivity layer is prominent in each of the models with its top at a depth of 20–25 km (pressures of 700–900 MPa) and extending south of the Indus–Tsangpo suture. The MT data can also be fitted by other resistivity

[1]Department of Physics, University of Alberta, Edmonton, Alberta, T6G 2J1, Canada. [2]School of Cosmic Physics, Dublin Institute for Advanced Studies, 5 Merrion Square, Dublin 2, Ireland. [3]Geo-detection Laboratory, Ministry of Education, China University of Geosciences, 29 Xueyuan Road, Beijing 100083, China. [4]EOST-IPGS, EOST ULP (UMR-7516), 5 rue Rene Descartes, University of Strasbourg, Strasbourg 67084, France. [5]Indian Institute of Geomagnetism, Colaba, Mumbai 400005, India.
*Lists of participants and affiliations appear at the end of the paper.

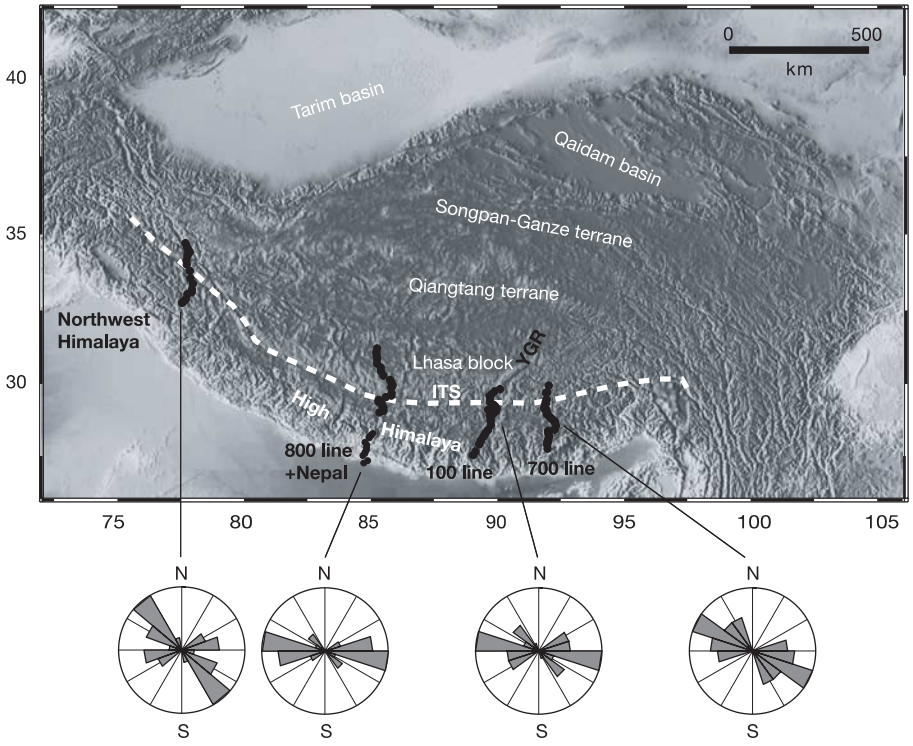

Figure 1 | Map of the Tibetan plateau showing the location of the MT profiles. The rose diagrams show geoelectric strike directions derived from the MT data using tensor decomposition. The scatter is typical of this type of data. ITS, the Indus–Tsangpo suture.

models, with the same ratio of resistivity and layer thickness. In Fig. 2 the thickest possible layer is chosen, and this corresponds to the lowest fluid fraction. The profile in the northwest Himalaya is characterized by higher mid-crustal resistivities than in southern Tibet. Differences between the models in Fig. 2 are not due solely to subsurface structure. Deep MT exploration uses natural electromagnetic signals that are variable from year to year with the solar cycle. Long-period (<1 Hz) signal levels were low in 1995 when the 100 line was recorded and high in 2001 close to the sunspot maximum when the 700 and 800 lines were recorded. The profile in the northwest Himalaya used only broadband instruments and signal penetration was shallower. Thus the models in Fig. 2 reflect that deepest signal penetration was achieved on the 700 line. An independent analysis[21] of the 100- and 700-line data yielded models with essentially the same primary features as in Fig. 2.

What is the origin of the low-resistivity layer? The 100 line is coincident with the INDEPTH seismic reflection profile (Fig. 3) with the Main Himalayan Thrust interpreted as the top of the underthrusting Indian plate[11]. An increase in resistivity is observed at the depth of the Main Himalayan Thrust, as expected for the cold Indian

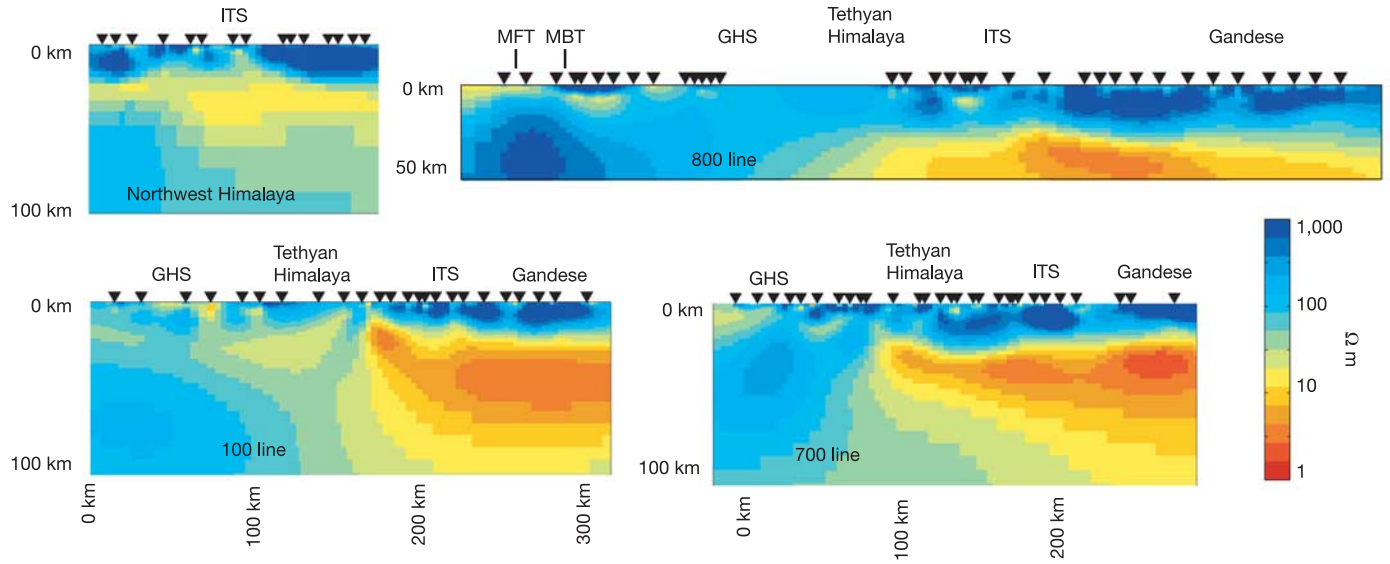

Figure 2 | Resistivity models for the four profiles derived from inversions of the MT data. The control parameters were varied to ensure that the final models were well defined. The MT data are fitted to a root-mean-square (r.m.s.) misfit in the range 1.5 and 2.5, which is statistically acceptable. Static shifts were removed from the data by allowing the inversion algorithm to estimate the coefficients. Other approaches were used and gave consistent results. Inverted triangles denote the locations of the MT stations. MFT, Main Frontal Thrust, MBT, Main Boundary Thrust; GHS, Greater Himalayan Sequence.

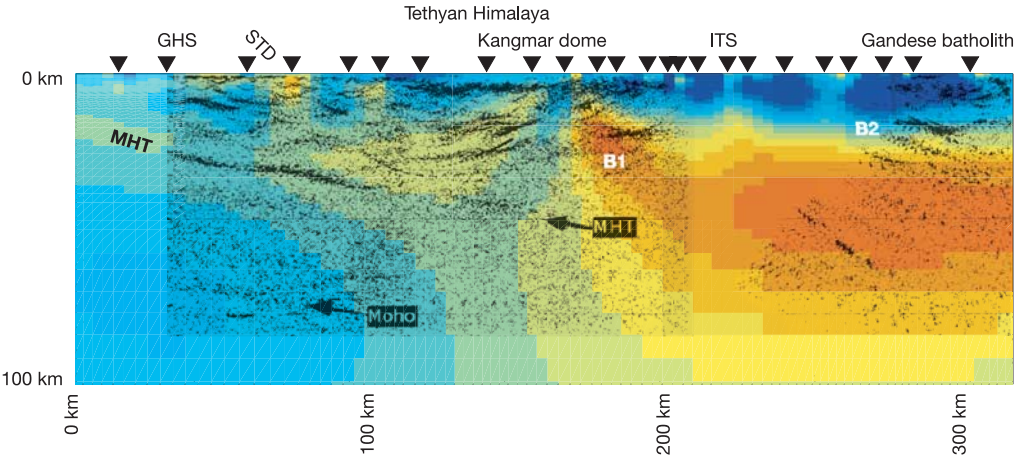

Figure 3 | Comparison of 100-line resistivity model and the INDEPTH common mid-point reflection profile. B1 and B2 are seismic bright spots that indicate zones with high fluid content. MHT, Main Himalayan Thrust; STD, Southern Tibetan detachment. Moho, Mohorovic discontinuity.

lithosphere. The Main Himalayan Thrust reflection disappears where the low-resistivity layer begins in the Tibetan mid-crust (along-profile distance of 160 km). This can be explained if the mid-crustal layer represents a zone of high fluid content, because seismic energy will be attenuated by a fluid layer. The top of the low-resistivity layer is coincident with seismic bright spots (B1 and B2) whose seismic characteristics suggest they contain significant amounts of fluids.

The nature of these fluids is still debated, with partial melt and/or aqueous fluids as the most likely, and least contrived, explanations. Seismic reflection data suggest that the top of this layer could be aqueous fluids[22], while surface wave studies suggest a broader zone characteristic of partial melting[11]. Aqueous fluids lower the melting point of the crust and, combined with the increased heat flow in southern Tibet[13], could cause partial melting at depths of 20–30 km (ref. 8). Thus a combination of aqueous fluids overlying a layer of partial melting gives the most consistent explanation of both the MT and seismic data[22,23]. In addition, the geometry of the low-resistivity layer is consistent with the geometry of the zone of partial melting predicted by geodynamic models[8]. The southern edge of this zone is 50–100 km south of the Indus–Tsangpo suture and at a depth of 20–30 km. Laboratory measurements of the resistivity of hydrous granite melts gives further evidence that conditions for crustal melting occur beneath southern Tibet[24]. Assuming that the low resistivity is primarily due to partial melting, the melt fraction was computed assuming good interconnection[25] and a pure melt resistivity of 0.1–0.3 Ω m (ref. 23). A bulk resistivity of 3 Ω m, typical of southern Tibet, requires a melt fraction in the range 5–14% (Fig. 4a).

Crustal flow requires a layer with a viscosity lower than the adjacent rocks and an effective viscosity below an absolute threshold that is dependent on the layer thickness. It was once believed that a melt fraction in excess of 30% was required to substantially lower the viscosity of crustal rock[26]. However, a reexamination of laboratory data suggests that a larger, absolute reduction in viscosity occurs with a melt fraction in the range 0–7%, as the melt forms an interconnected network[27,28,29]. When a sample of aplite was 5–7% molten, the effective viscosity was reduced by an order of magnitude[29]. This is the amount required for strain localization and flow in geodynamic models of southern Tibet[8].

Are these conditions encountered in Southern Tibet? The MT data require a melt fraction of 5–14%, which is sufficient to produce an order-of-magnitude reduction in viscosity and an absolute viscosity below the values necessary to account for the topography[30] of the Tibetan plateau (10^{16} to 10^{18} Pa s). The decrease in viscosity for granite[28] at these melt fractions is less, and perhaps insufficient for crustal flow to develop. It must also be noted that the extrapolation of laboratory experiments (Fig. 4b) to the low strain rates encountered in crustal deformation can be ambiguous. A similar analysis for the northwest Himalaya yields melt fractions of 2–4% that correspond to a more modest reduction in viscosity and a less-well-developed crustal flow.

The observation of a low-viscosity mid-crustal layer has a number of geodynamic consequences. A weak layer effectively decouples the upper and lower parts of the Tibetan crust, allowing east–west

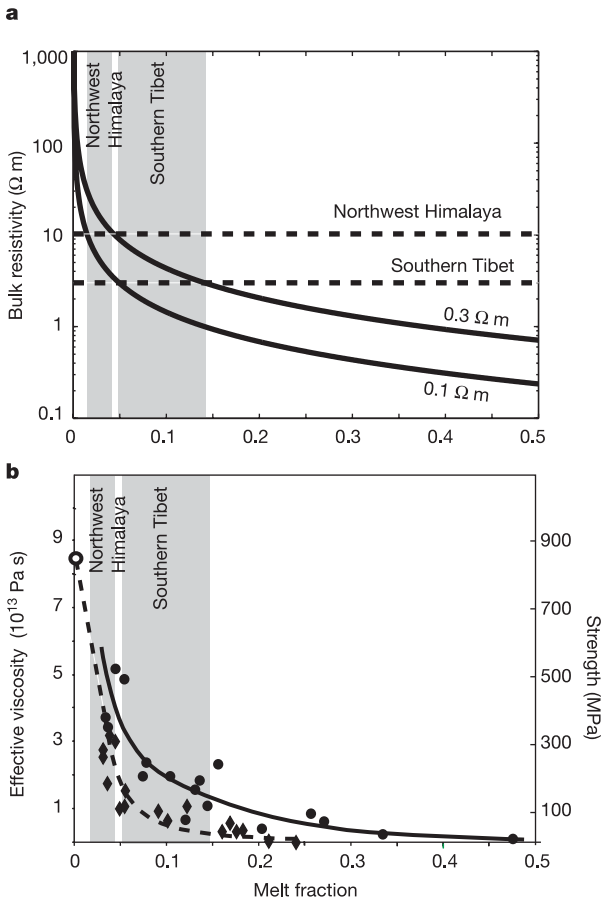

Figure 4 | Summary of laboratory measurements of the electrical resistivity and mechanical properties of a partially molten rock. a, Bulk electrical resistivity of partial melts as a function of melt fraction for melt resistivities of 0.1 and 0.3 Ω m; **b**, effective viscosity and strength of Westerly granite (circles) and aplite (diamonds) as a function of melt fraction[27]. Error bars are not shown, and solid and dashed lines show best-fitting trends for Westerly granite[28] and aplite[29]. The strength was computed for a strain rate of 10^{-5} s^{-1}.

extension at the surface while convergence continues at depth. The Yadong–Gulu rift[15] appears to have little effect on the amount of fluid in the crust, and is probably a passive feature that has formed in response to deformation in the mid-crust. The lowest melt fractions are inferred in the northwest Himalaya, far from the extruding eastern margin of Tibet. This might be due to slower crustal motion in this area, or reflect a lower input of radiogenic heat in the underthrust rock units. There is some indication that the inferred flow may be episodic in time. Bright spot B1 probably represents an accumulation of melt, and the resistive break south of B1 may represent recently crystallized granite.

In addition to the inferred crustal flow in Southern Tibet, a larger-scale southward and eastward crustal flow may occur in northern and eastern Tibet[30]. MT data collected in these areas have imaged zones of low crustal resistivity that may represent regions of low viscosity[14].

Received 7 March; accepted 16 August 2005.

1. Yin, A. & Harrison, T. M. Geologic evolution of the Himalayan-Tibetan orogen. *Annu. Rev. Earth Planet. Sci.* **28,** 211–280 (2000).
2. Argand, E. in *Proceedings of the 13th International Geological Congress* 170–372 (Brussels, 1924).
3. Dewey, J. F. & Burke, K. A. Tibetan, Variscan and Precambrian Basement reactivation: products of continental collision. *J. Geol.* **81,** 683 (1973).
4. Tapponnier, P. *et al.* Oblique stepwise rise and growth of the Tibetan Plateau. *Science* **294,** 1671–1677 (2001).
5. Molnar, P., England, P. & Martinod, J. Mantle dynamics, uplift of the Tibetan Plateau and the Indian monsoon. *Rev. Geophys.* **31,** 357–396 (1993).
6. Le Fort, P. *et al.* Crustal generation of the Himalayan leucogranites. *Tectonophysics* **134,** 39–57 (1987).
7. Grujic, D., Hollister, L. S. & Parrish, R. R. Himalayan metamorphic sequence as an orogenic channel: insight from Bhutan. *Earth Planet. Sci. Lett.* **198,** 177–191 (2002).
8. Beaumont, C., Jamieson, R. A., Nguyen, M. H. & Lee, B. Himalayan tectonics explained by extrusion of a low-viscosity crustal channel coupled to focused surface denudation. *Nature* **414,** 738–742 (2001).
9. Lee, J. *et al.* Evolution of the Kangmar Dome, southern Tibet: Structural, petrologic, and thermochronologic constraints. *Tectonics* **19,** 872–895 (2000).
10. Owens, T. J. & Zandt, G. Implications of crustal property variations for models of Tibetan plateau evolution. *Nature* **387,** 37–43 (1997).
11. Nelson, K. D. *et al.* Partially molten middle crust beneath southern Tibet: synthesis of project INDEPTH results. *Science* **274,** 1684–1687 (1996).
12. Pham, V. N. *et al.* Partial melting zones in the crust in Southern Tibet from magnetotelluric results. *Nature* **319,** 310–314 (1986).
13. Francheteau, J. *et al.* High heat-flow in southern Tibet. *Nature* **307,** 32–36 (1984).
14. Wei, W. *et al.* Detection of widespread fluids in the Tibetan crust by magnetotelluric studies. *Science* **292,** 716–718 (2001).
15. Armijo, R., Tapponnier, P., Mercier, J. L. & Han, T. L. Quaternary extension in southern Tibet; field observations and tectonic implications. *J. Geophys. Res.* **91,** 13803–13872 (1986).
16. Jones, A. G., Chave, A. D., Auld, D., Bahr, K. & Egbert, G. A comparison of techniques for magnetotelluric response function estimation. *J. Geophys. Res.* **94,** 14201–14213 (1989).
17. Lemmonier, C. *et al.* Electrical structure of the Himalaya of Central Nepal: high conductivity around the mid-crustal ramp along the Main Himalayan Thrust. *Geophys. Res. Lett.* **26,** 3261–3264 (1999).
18. Gokarn, S. G., Gupta, G., Rao, C. K. & Selvaraj, C. Electrical structure across the Indus Tsangpo suture and Shyok suture zones in NW Himalaya using magnetotelluric studies. *Geophys. Res. Lett.* **29,** 1–4 (2002).
19. McNeice, G. M. & Jones, A. G. Multisite, multifrequency tensor decomposition of magnetotelluric data. *Geophysics* **66,** 158–173 (2001).
20. Rodi, W. & Mackie, R. L. Nonlinear conjugate gradients algorithm for 2-D magnetotelluric inversion. *Geophysics* **66,** 174–187 (2001).
21. Spratt, J., Jones, A. G., Nelson, K. D., Unsworth, M. J. & the INDEPTH MT team. Crustal structure of the India-Asia collision zone, southern Tibet, from INDEPTH MT investigations. *Phys. Earth Planet. Inter.* **150,** 227–237 (2005).
22. Makovsky, Y. & Klemperer, S. L. Measuring the seismic properties of Tibetan bright spots: Evidence for free aqueous fluids in the Tibetan middle crust. *J. Geophys. Res.* **104,** 10795–10825 (1999).
23. Li, S. *et al.* Partial melt or aqueous fluids in the Tibetan crust: constraints from INDEPTH magnetotelluric data. *Geophys. J. Int.* **153,** 289–304 (2003).
24. Gaillard, F., Scaillet, B. & Pichavant, M. Evidence for present-day leucogranite pluton growth in Tibet. *Geology* **32,** 801–804 (2004).
25. Schilling, F. R., Partzsch, G. M., Brasse, H. & Schwarz, G. Partial melting below the magmatic arc in the central Andes deduced from geoelectromagnetic field experiments and laboratory data. *Phys. Earth Planet. Inter.* **103,** 17–31 (1997).
26. Renner, J., Evans, B. & Hirth, G. On the rheologically critical melt fraction. *Earth Planet. Sci. Lett.* **181,** 585–594 (2000).
27. Rosenberg, C. & Handy, M. R. Experimental deformation of partially melted granite revisited: implications for the continental crust. *J. Metamorph. Geol.* **23,** 19–28 (2005).
28. Rutter, E. & Neumann, D. H. K. Experimental deformation of partially molten Westerly granite under fluid absent conditions with implications for the extraction of granitic magmas. *J. Geophys. Res.* **100,** 15697–15715 (1995).
29. Van der Molen, I. & Paterson, M. S. Experimental deformation of partially molten granite. *Contrib. Mineral. Petrol.* **70,** 299–318 (1979).
30. Clark, M. K. & Royden, L. H. Topographic ooze: Building the Eastern margin of Tibet by lower crustal flow. *Geology* **28,** 703–706 (2000).

Supplementary Information is linked to the online version of the paper at www.nature.com/nature.

Acknowledgements The MT data were collected and analysed with support from the US National Science Foundation, the Ministry of Land and Resources of China, the Ministry of Education of China, the National Science Foundation of China, NSERC (Canada) and the Alberta Ingenuity Fund. Data in India were collected with funding from the ESS Division, Department of Science and Technology, Government of India, under the Deep Continental Studies Program. Data acquisition in Nepal was supported by CNRS-INSU and by the French-Nepalese cooperation agreement. Discussions with M. Edwards, W. Kidd and D. Nelson are acknowledged. We dedicate this paper to the memory of Doug Nelson, who inspired us all.

Author Information Reprints and permissions information is available at npg.nature.com/reprintsandpermissions. The authors declare no competing financial interests. Correspondence and requests for materials should be addressed to M.J.U. (unsworth@phys.Ualberta.ca).

The INDEPTH-MT team Paul Bedrosian[1], John Booker[2], Chen Leshou[3], Greg Clarke[4], Li Shenghui[2], Lin Chanhong[3], Deng Ming[3], Jin Sheng[3], Kurt Solon[5], Tan Handong[3], Juanjo Ledo[6] & Brian Roberts[7]

Affiliations for participants: [1]United States Geological Survey, ICT, MS964, Box 25046, Denver, Colorado 80225, USA. [2]Department of Earth and Space Sciences, University of Washington, Seattle, Washington 98195, USA. [3]Department of Applied Geophysics, China University of Geosciences, Beijing 100083, China. [4]Department of Earth Sciences, University of Western Ontario, London, Ontario N6A 5B7, Canada. [5]Geological Sciences, Syracuse University, Syracuse, New York 13244, USA. [6]Departament de Geodinàmica i Geofísica, Facultat de Geologia, Universitat de Barcelona, Martí i Franques s/n, 08028 Barcelona, Spain. [7]Geological Survey of Canada, 615 Booth Street, Ottawa, Ontario K1A 0E9, Canada.